First Title Page

Title:

Preliminary study on evaluation of the pancreatic tail observable limit of transabdominal ultrasonography using a position sensor and CT-fusion image

Authors:

Hajime Sumi, MD[1)], Akihiro Itoh, MD, PhD[1)], Hiroki Kawashima, MD, PhD[1)], Eizaburo Ohno, MD, PhD[2)], Yuya Itoh, MD[1)], Yosuke Nakamura, MD[1)], Takeshi Hiramatsu, MD[1)], Hiroyuki Sugimoto, MD[1)], Daijuro Hayashi, MD[1)], Takamichi Kuwahara, MD[1)], Tomomasa Morishima, MD[1)], Manabu Kawai, MD[1)], Kazuhiro Furukawa, MD, PhD[1)], Kohei Funasaka, MD, PhD[2)], Masanao Nakamura, MD, PhD[1)], Ryoji Miyahara, MD, PhD[1)], Yoshiaki Katano, M.D., PhD[3)], Masatoshi Ishigami M.D. PhD[1)], Naoki Ohmiya, MD, PhD[3)], Hidemi Goto, MD, PhD[1) 2)], and Yoshiki Hirooka, MD PhD[2)]

Affiliations:

1) Department of Gastroenterology and Hepatology Nagoya University Graduate

School of Medicine, Nagoya, Japan

2) Department of Endoscopy, Nagoya University Hospital, Nagoya, Japan

3) Department of Gastroenterology, Second Teaching Hospital, Fujita Health University, Japan

The corresponding author: Yoshiki Hirooka

Department of Endoscopy, Nagoya University Hospital, Nagoya

65 Tsuruma-cho, Showa-ku, Nagoya City, 466-8550, Japan

Phone: +81 (52) -744-2602, Fax: +81 (52) -735-8806

E-mail; hirooka@med.nagoya-u.ac.jp

Abstract

Background and aim: Transabdominal ultrasonography (US) is commonly used for the initial screening of bilio-pancreatic diseases in Asian countries due to its widespread availability, the non-invasiveness and the cost-effectiveness. However, it is considered that US has limits to observe the area, namely the blind area. The observation of the pancreatic tail is particularly difficult. The goal of this study was to examine the pancreatic tail region that cannot be visualized on transverse scanning of the upper abdomen using US with spatial positional information and factors related to visualization, and observation of the tail from the splenic hilum.

Methods: Thirty-nine patients with pancreatic/biliary tract disease underwent CT and US with GPS-like technology and fusion imaging for measurement of the real pancreatic length and the predicted/real unobservable (PU and RU) length of the pancreatic tail. RU from US on transverse scanning and the real pancreatic length were used to determine the unobservable area (UA: RU / the real pancreatic length). Relationships of RU with physical and hematological variables that might influence visualization of the pancreatic tail were investigated.

Results: The real pancreatic length was 160.9±16.4 mm, RU was 41.0±17.8 mm, and UA was 25.3±10.4%. RU was correlated with BMI (R=0.446, P=0.004) and waist circumferences (R=0.354, P=0.027), and strongly correlated with PU (R=0.788, P<0.001). The pancreatic tail was visible from the splenic hilum in 22 (56%) subjects and was completely identified in 13 (33%) subjects.

Conclusions: Combined GPS-like technology with fusion imaging was useful for the objective estimation of the pancreatic blind area.

Keywords

Blind area of pancreas image; Transabdominal ultrasonography (US); Fusion image of CT and US; GPS-like technology

1. Introduction

Transabdominal ultrasonography (US) is still considered useful for the initial screening, medical examinations and general clinical practice in Japan and other countries because of its convenience, non-invasiveness, cost-effectiveness and real-time imaging [1, 2]. In fact, US is commonly used as first choice for biliary and pancreatic disease in particularly Asian countries, so that US plays a key role. Recent developments in technology including tissue harmonic imaging and contrast harmonic imaging have improved the spatial resolution and contrast resolution of US [3-7]. US allows real-time imaging, but is examiner-dependent and has limited objectivity. Thus, methods for synchronization of US with other imaging methods in real time (fusion imaging), and functions that marks a region of interest (ROI) and track a spatial point (global positioning system (GPS)-like technology) have been developed and may be useful for navigation in percutaneous radiofrequency ablation (RFA) in liver tumor treatment [8-13]. These functions facilitate positioning in US and improve the objectivity. On the other hand, it is still difficult to observe the pancreatic tail by US and tumors in the pancreatic tail may not be found until an advanced stage in which the patient feels ill and visits a hospital. It is because of the limits of US, namely a blind area due to the presence of intestinal gas and fat. It is essential that US examiners precisely recognize the pancreas area that can be covered using US. However, an objective study of the blind area in visualization of the pancreatic tail on US has not been performed. Therefore, we investigated factors that influence visualization of the pancreatic tail using US with GPS-like technology and fusion imaging.

2. Materials and methods

2.1. Patients

The subjects were 39 patients (male: 21, female: 18, 36 to 80 years old, mean age: 62.8 years old) out of 61 consecutive patients with pancreatic/biliary tract disease who were hospitalized for examination and underwent multidetector-row computed tomography (MDCT) and US with GPS-like technology and fusion imaging between November 2011 and January 2013. Of the 61 patients, 22 met the following exclusion criteria that might influence observation of the pancreatic tail: (1) lesion in the pancreatic tail, (2) atrophic change of the pancreatic tail, (3) dilation of the main pancreatic duct >5 mm, (4) chronic pancreatitis with stones, (5) unobservable spleen, (6) abdominal surgery, and (7) ascites. Of the 39 subjects, 14 had a tumor in the pancreatic head and

body, 13 had a duodenal papillary tumor (including disease treated with endoscopic therapy), 2 had a duodenal tumor, 8 had gallstone cholecystitis and gallbladder cancer, 1 had chronic pancreatitis, and 1 had hilar cholangiocarcinoma. Detail characteristics of the 39 patients are shown in Table 1.

Physical and hematological factors that might influence visualization of the pancreatic tail were examined on admission. The physical variables included age, height, body mass index (BMI) and waist circumference; and the hematology data were indicators for glucose and lipid metabolism, total protein (TP), albumin (Alb), cholinesterase (ChE), triglyceride (TG), total cholesterol (T-C), low density lipoprotein cholesterol (LDL-C), high density lipoprotein cholesterol (HDL-C), free fatty acid (FFA) and glycosylated hemoglobin (HbA1c) [14-16]. Waist circumference was defined as the paraumbilical circumference based on NCEP-ATIII [17] and AHA/NHLBI [18] guidelines.

After routine US, the real pancreatic length and the blind area of the pancreas were investigated using US with GPS-like technology and CT-fusion imaging. Subsequently, factors related to the area that could not be visualized by routine US and observation of the pancreatic tail from the splenic hilum were evaluated. US was performed by a single experienced examiner with the patient in a supine position with the hands above the head. Written informed consent was obtained from all patients. This study was approved by IRB (institutional review board) of our hospital and registered as No. 000009285 at UMIN-CTR (University hospital Medical Information Network – Clinical Trials Registry).

2.2. Definition of terms

The non-visible region of the pancreatic tail by US in transverse scanning of the upper abdomen (transverse scanning) was defined as the real unobservable length of the pancreatic tail (RU). The ratio of RU to the real pancreatic length was defined as the unobservable area (UA). The pancreatic tail end visualized by transverse scanning was defined as the target point (TP). To estimate RU by US with GPS-like technology, but not fusion imaging, the length from TP to the splenic hilum region was defined as the predictive length of the unobservable area (PU). For simplicity, TP and PU were labeled as TP-US/CT and PU-US/CT (depending on the image on which TP marked or PU measured).

2.3. Equipment and volume navigation system

Ultrasonography was performed using a Logic E9 system (GE Healthcare) (**Fig. 1**) and a transmitter generating magnetic fields set on the bedside close to the left hypochondriac region. The probe was the convex type for the abdomen (4 MHz, C1-5) with an attachment for installation of two magnetic sensors. The probe position and direction were detected in real time by detecting the transmitter-generated magnetic field with a sensor installed in the probe. CT data obtained by MDCT prior to the study were transferred to the ultrasonograph system in accordance with digital imaging and communication in medicine (DICOM) guidelines. Positional information for the ultrasonic probe and volume data corresponding to this information were reconstructed as CT-multiplanar reconstruction images using the volume navigation (V-Nav) built-in software. This allowed display of CT images in parallel to the right of the US image in real time (frame rate >10 /s) (fusion imaging technique) and GPS-like technology to track the spatial point. Registration is done by defining a common plane plus one additional, common point.

The fusion imaging technique displays a real-time US image on the left and a CT-MPR image synchronized with the US image on the right. Spatial positioning is achieved using a GPS marker on the screen that indicates the accuracy. The marker is displayed as a large square if it is distant from the correct position, as a small square if closer, and as a cross if it corresponds exactly with the correct position (**Fig. 2a**). The marker is displayed on the US and CT images. CT volume data in 0.5-mm slices were used to facilitate recognition of the pancreatic parenchyma using 64-slice MDCT with iohexol.

2.4. Measurement of the length of the pancreas

The real pancreatic length was measured using US with GPS-like technology and CT-fusion imaging. The length of the pancreatic head and pancreatic body and tail were measured in CT cross-sectional images. The junction (confluence) of the superior mesenteric and splenic vein was identified by transverse scanning in CT-fusion images. The pancreatic parenchyma on the abdominal side was visualized and a GPS marker was positioned at the center of the pancreatic parenchyma on the left margin of the portal vein in the CT-fusion image. The GPS marker was also displayed on the US image (**Fig. 2b**). Next, in the CT fusion image showing the papillary region in which the pancreatic duct joined the common bile duct, the probe position, degree and rotation were manipulated to change the square GPS marker into a cross. The length from the marker to the papillary region (pancreatic head length: A) was then measured (**Fig. 2c**). Display of the GPS marker as a cross indicates accurate spatial positioning of the marker on the US and CT images, although the probe position and direction differ from those of the images. Subsequently, the pancreatic tail end was visualized on the CT-fusion image and the length from the marker to the pancreatic tail

end (pancreatic body and tail length: B) was measured while maintaining the marker as a cross (**Fig. 2d**). The total length of A and B was defined as the real pancreatic length.

2.5. Measurement of the blind area of the pancreas

In transverse scanning, the pancreatic end visualized by US was defined as the target point (TP) and marked on the US image using GPS-like technology (**Fig. 2e**). TP-US marked on the US image was also marked on the corresponding CT-fusion image (TP-CT), thus allowing the position of a region that could be visualized by US to be confirmed in the CT-fusion image. In observation of the pancreatic tail from the splenic hilum by left intercostal scanning, the marker indicated the spatial position in US and CT-fusion images and the TP position marked in observation of the pancreatic tail by transverse scanning were confirmed. The pancreatic tail that could not be visualized by US in transverse scanning was confirmed by left intercostal scanning using CT-fusion imaging and the distance from TP-CT to the pancreatic tail end (RU) was measured on the CT-fusion image (**Fig. 2f①**). Similarly, the distance from TP-US to the splenic hilum region (PU-US) was measured on the US image (**Fig. 2f②**) and that from TP-CT to the splenic hilum (PU-CT) was measured on the CT-fusion image (**Fig. 2f③**). The ratio of RU to the real pancreatic length (UA) was calculated from these data.

To evaluate the effect of pancreatic duct dilation on visualization of the pancreatic tail, the subjects were divided into two groups based on the maximum diameter of the main pancreatic duct: i.e., those with a maximum diameter >3 mm in the pancreatic body and tail were considered to have pancreatic duct dilation. The accuracy of the CT-fusion imaging technique was also evaluated by comparing PU-US in US images with PU-CT in CT-fusion images, and the mean and range of absolute differences were measured.

2.6. Visualization of the pancreatic tail by left intercostal scanning

Generally, visualization of the pancreatic tail from the splenic hilum region is necessary to detect a targeted-lesion in the pancreatic tail. The effectiveness of this visualization in US was evaluated based on classification of images into three groups in which the pancreatic tail (a) could be identified between TP-US and the splenic hilum, (b) could not be identified clearly, but was suspected to present, and (c) could not be observed due to intestinal gas (**Fig. 3**). A targeted-lesion in the pancreatic tail is often

visible although the pancreatic tail itself cannot be identified. Therefore, cases in categories (a) and (b) were considered to be positive for visualization of the pancreatic tail, whereas those in (c) were negative.

2.7. Reevaluation of the location of TP and classification of visualization of the pancreatic tail

The validity of the TP position and the classification of visualization of the pancreatic tail from the splenic hilum region into 3 groups were reevaluated by two gastroenterologists with more than 10 years of experience in US (estimators). Only the US image of the pancreatic tail obtained by transverse scanning was given to the estimators and the limit of visualization of the pancreatic tail (TP of the estimators) was marked by the estimators. The distances between the marks (yellow and red) of the two estimators and the cross mark (green) of the examiner were measured perpendicular to the direction of the long axis (**Fig. 4**). When TP of the examiner was set at 0, the distances to the papillary region and tail were regarded to be positive and negative, respectively. RU of the estimators was determined by adding the difference in the distance between TP of the estimators and TP of the examiner. The consistency of RU between the examiner and two estimators was evaluated to estimate the reliability of TP of the examiner. To examine visualization of the pancreatic tail from the splenic hilum region, US images from this region were given to the estimators, classified into 3 categories, and accepted if at least 2 of 3 persons (an examiner and two estimators) had the same classification, but considered unobservable if all 3 persons had different evaluations.

2.8. Statistical analysis

Factors related to RU were evaluated by Pearson test for data with a normal distribution and by Spearman test for those with a non-normal distribution. Means of variables were compared based on sex, the presence or absence of pancreatic duct dilation, and PU-US and PU-CT by *t* test and Mann-Whitney *U* test. To evaluate the reliability of TP between one examiner and two estimators, an intraclass correlation coefficient (ICC) (2, 3) was used for the consistency of RU among 3 persons using the criteria of Landis et al. [19]: $r < 0$, no agreement; 0-0.20, slight agreement; 0.21-0.40, fair agreement; 0.41-0.60, moderate agreement; 0.61-0.80, substantial agreement; and 0.81-1.0, almost perfect agreement. Analyses were performed in SPSS ver.20 and $P < 0.05$ was taken to indicate a significant difference.

3. Results

There were significant sex differences in height and weight, and HDL-C was significantly higher in females. There were no significant differences in age, BMI, waist circumference and other hematological parameters. The mean length of the pancreas, RU, UA, PU-US, and PU-CT are shown in Table 2. The mean length of the pancreas was 160.9±16.4 mm (128-203 mm), the mean RU was 41.0±17.8 mm, and the mean UA was 25.3±10.4%; i.e., about 25% of the length of the pancreas could not be visualized. The pancreas tended to be longer in males, but with no significant difference. There was also no sex difference in RU and UA, but PU-US and PU-CT were significantly longer in males.

Slight pancreatic duct dilation was present in 10 subjects. Physical findings and US findings did not differ significantly between patients with and without pancreatic duct dilation. RU had correlations with BMI (R=0.446, P = 0.004) and waist circumference (R=0.354, P = 0.027), but no correlations with hematology data (**Fig. 5**). The mean values of PU-US and PU-CT did not differ significantly (0.6 mm). The mean absolute difference between PU-US and PU-CT was 4.3 mm (range: 0-16.6 mm). PU-US had a strong correlation with RU (R=0.788, P < 0.001; linear regression equation: y = 0.887x-5.125, R^2 = 0.62). RU was estimated from PU-US. PU-US was 52.0±15.8mm and was longer than RU by about 1 cm. The confidence coefficient of RU among the 3 persons (the examiner and two estimators) was r = 0.926, indicating almost perfect agreement.

The pancreatic tail was observable by left intercostal scanning in 56% (22/39) of the subjects and could be completely identified in 33% (13/39) (Table 3). A comparison of variables between subjects in whom the pancreatic tail was and was not observable showed that TG was significantly higher in the observable group with Mann-Whitney U test.

The results of this study showed that RU (real unobservable length of pancreatic tail) was about 40 mm and that about 25% of the pancreas could not be visualized in US. RU was positively correlated with BMI and waist circumference.

4. Discussion

US is a simple method with non-invasiveness that has become increasingly useful for lesion detection due to developments in technology. US can be used for real-time observation of hemodynamics with contrast agents and observation of lesion hardness with the elastography technique, which open up the possibility of using US for qualitative diagnosis [3-7, 20]. However, some regions are unobservable in US and the pancreatic tail is a particularly problematic region due to the presence of intestinal gas and

fat. US is useful for lesions in the pancreatic head and body by direct visualization of the tumor and indirect findings of pancreatic duct dilation and biliary dilation. However, it is difficult to visualize lesions in the pancreatic tail using US, in contrast to CT and MRI. The invisible area in the pancreatic tail on US has not been examined previously and detection of the pancreatic limit of US is important for objective evaluation of visualization of the pancreatic tail.

In this study, GPS-like technology and CT-fusion imaging were used for objective evaluation of visualization of the pancreatic tail by US. The fusion image technique provides objectivity in US and may be useful in RFA therapy for liver cancer [8-13]. This technique is particularly useful for sites that are difficult to observe by US and for lesions that cannot be visualized, and is also useful in other fields [21-23]. Nakano et al. [22] showed that the sensitivity for preoperative detection of breast tumors by MRI and real-time virtual sonography was better than that for US or MRI alone, and Khalil et al. [23] found that US fusion in CT-guided biopsy improved diagnostic performance and the accuracy of bone tumor detection, with a consequent reduction in biopsy time. These results were obtained by fusion techniques that enhanced the advantages of imaging modalities and compensated for weaknesses. Basic and clinical studies have shown the accuracy of GPS-like technology and image fusion [12, 24, 25]. Schlaier et al. [24] found fusion accuracy of 1.08±0.61 mm, and Kitada et al. [12] showed that the error between a puncture line and the tumor center in RFA therapy was 1.6 mm.

In visualizing the pancreatic tail by transverse scanning, compression of the abdominal wall may cause differences in location on CT. However, a deep organ such as the pancreas has less positional change than the body surface. Sofuni et al. [26] evaluated the usefulness of CT fusion imaging in the field of biliary and pancreatic diseases. The difference between the mean PU-US and PU-CT was only 0.6 mm and the mean absolute difference was 4 mm, which was slightly lower in accuracy than that in previous studies. This difference is due to the large change in the pancreatic tail position due to respiration. PU-US and PU-CT were significantly longer in males than in females, and the length of the pancreas tended to be longer in males, but with no significant difference. There is more visceral fat in men and this may have an effect on PU.

US is also considered to be less objective due to technical differences among examiners. TP in examination of the pancreatic tail depended on observers and TP of the estimators differed in the current study. To evaluate the TP validity, the difference between TP of the examiner and the points marked by the two estimators was measured and RU was estimated. Using ICC (2, 3), the confidence coefficient was $r = 0.926$, indicating that the TP position of the examiner was valid.

The mean pancreatic length in our subjects was 160.9±16.4 mm (128-203 mm). Wilasrusmee et al. [27] examined the pancreatic and bile duct and the pancreatic form in autopsy specimens of 103 Thai patients with a cause of death unrelated to

trauma or pancreatic/biliary tract disease. The mean directly measured pancreatic length was 156±18mm (109-190 mm), which was similar to that in our study. In measurements in healthy men using CT cross-sectional images, Schulz et al. [28] found a mean pancreatic length of 129.3±16 mm, which was shorter than that in our study. The pancreas is not linear, since the head expands vertically and the body extends leftward, followed by the tail in the direction of the left back side with a further slope. Therefore, the length may be shorter in simple CT. Pochhammer et al. [29] found a pancreatic length of 80 mm visualized by US but unobservable area was not mentioned. The results of this study showed that RU was about 40 mm and that about 25% of the pancreas could not be visualized in US. RU was positively correlated with BMI and waist circumference, but not with obesity-related hematological findings. Halle et al. [16] found significant differences in TG and subfractions of lipoprotein levels, but not in total LDL-C and HDL-C at BMI≥25. In the current study, 12 subjects had BMI≥25, but the lipoprotein fraction of LDL-C and HDL-C was not evaluated. TG had no correlation with RU, but TG was significantly lower in subjects in whom the pancreatic tail could not be visualized by left intercostal scanning. These results suggest an effect of lean body type on visualization, but an effect of pancreatic/biliary tract disease on lipid metabolism also cannot be ruled out.

In clinical practice, it is difficult to know the extent to which the pancreatic tail can be observed by US. GPS-like technology requires no preparation in advance and is easy to use simultaneously with US; therefore, PU is useful for prediction of RU. Furthermore TP might be useful of early detection of the tumor of the pancreatic tail because it is easier to predict the location of the pancreatic tail in visualization by left intercostal scanning, even though the pancreatic tail cannot be identified.

The study has several limitations. First, the result of this study was limited by the small patient sample size. The outcome obtained from this study showed the preliminary information for observable limits of the pancreas using US in clinical practice. Larger number of patients' data are necessary to confirm our data. Second, CT images were collected in a supine position and visualization of the pancreatic tail may be improved by postural changes. Lastly, contrast-enhanced CT was conducted in patients due to ethical considerations and the subjects were elderly; therefore, the results may not correspond to those in healthy younger persons. Thus, despite this study's limitations, this is the first investigation of the visibility of the pancreatic tail using US with GPS-like technology and CT-fusion imaging.

5. Conclusion

Combined GPS-like technology with fusion imaging gave the basic information essential in the examination of pancreas using

US. The clinical usefulness remains unclear and the validity of this technique requires further investigation.

Conflict of interest

The authors declare that they have no conflict of interest.

References

[1] Gandolfi L, Torresan F, Solmi L, Puccetti A. The role of ultrasound in biliary and pancreatic diseases. Eur J Ultrasound 2003;16(February (3)):141–59 [review].

[2] Fukumoto A, Tanaka S, Imagawa H, et al. Usefulness and limitations of transabdominal ultrasonography for detecting small-bowel tumors. Scand J Gastroenterol 2009;44(3):332–8.

[3] Matsuda Y, Yabuuchi I. Hepatic tumors: US contrast enhancement with CO_2 microbubbles. Radiology 1986;161:701–5.

[4] Hirooka Y, Itoh A, Kawashima H, et al. Contrast-enhanced endoscopic ultrasonography in digestive disease. J Gastroenterol 2012;47:1063–72.

[5] Ishikawa H, Hirooka Y, Itoh A, et al. A comparison of image quality between tissue harmonic imaging and fundamental imaging with an electronic radial scanning echoendoscope in the diagnosis of pancreatic diseases. Gastrointest Endosc 2003;57:931–6.

[6] Anderson CR, Hu X, Zhang H, et al. Ultrasound molecular imaging of tumor angiogenesis with an integrin targeted microbubble contrast agent. Invest Radiol 2011;46:215–24.

[7] Calliada F, Campani R, Bottinelli O, Bozzini A, Sommaruge MG. Ultrasound contrast agents: basic principles. Eur J Radiol 1998;27(Suppl. 2):S157–60.

[8] Jung EM, Schreyer AG, Schacherer D, et al. New real-time image fusion technique for characterization of tumor vascularisation and tumor perfusion of liver tumors with contrast-enhanced ultrasound, spiral CT or MRI: first results. Clin Hemorheol Microcirc 2009;43:57–69.

[9] Okamoto E, Sato S, Sanchez-Siles AA, et al. Evaluation of virtual CT sonography for enhanced detection of small hepatic nodules: a prospective pilot study. AJR 2010;194:1272–8.

[10] Ross CJ, Rennert J, Schacherer D, et al. Image fusion with volume navigation of contrast enhanced ultrasound (CEUS) with computed tomography (CT) or magnetic resonance imaging (MRI) for post-interventional follow-up after transcatheter

arterial chemoembolization (TACE) of hepatocellular carcinomas (HCC): preliminary results. Clin Hemorheol Microcirc 2010;46:101–15.

[11] Sandulescu DL, Dumitrescu D, Rogoveanu I, Saftoiu A. Hybrid ultrasound imaging techniques (fusion imaging). World J Gastroenterol 2011;17:49–52.

[12] Kitada T, Murakami T, Kuzushita N, et al. Effectiveness of real-time virtual sonography-guided radiofrequency ablation treatment for patients with hepatocellular carcinomas. Hepatol Res 2008;38:565–71.

[13] Jung EM, Friedrich C, Hoffstetter P, et al. Volume navigation with contrast enhanced ultrasound and image fusion for percutaneous interventions: first results. PLoS ONE 2012;7:e33956.

[14] Winocour PH, Kaluvya S, Ramaiya K, et al. Relation between insulinemia, body mass index, and lipoprotein composition in healthy, nondiabetic men and women. Arterioscler Thromb 1992;12:393–402.

[15] Xu W, Li R, Zhang S, et al. The relationship between high-sensitivity C-reactive protein and ApoB, ApoB/ApoA1 ratio in general population of China. Endocrine 2012;42:132–8.

[16] Halle M, Berg A, Frey I, König D, Keul J, Baumstark MW. Relationship between obesity and concentration and composition of low-density lipoprotein subfractions in normoinsulinemic men. Metabolism 1995;44:1384–90.

[17] Executive Summary of the Third Report of the National Cholesterol Education Program (NCEP) expert panel on detection, evaluation, and treatment of high blood cholesterol in adults (Adult Treatment Panel III). JAMA 2001; 285:2486–97.

[18] Grundy SM, Cleeman JI, Daniels SR, et al. Diagnosis and management of the metabolic syndrome: an American Heart Association/National Heart, Lung, and Blood Institute Scientific Statement. Circulation 2005;112:2735–52.

[19] Landis JR, Koch GG. The measurement of observer agreement for categorical data. Biometrics 1977;33:159–74.

[20] Athanasiou A, Tardivon A, Tanter M, et al. Breast lesions: quantitative elastography with supersonic shear imaging: preliminary results. Radiology 2010;256:297–303.

[21] Miyagawa T, Ishikawa S, Kimura T, et al. Real-time virtual sonography for navigation during targeted prostate biopsy using magnetic resonance imaging data. Int J Urol 2010;17:855–61.

[22] Nakano S, Yoshida M, Fujii K, et al. Fusion of MRI and sonography image for breast cancer evaluation using real-time virtual sonography with magnetic navigation: first experience. Jpn J Clin Oncol 2009;39:552–9.

[23] Khalil JG, Mott MP, Parsons TW 3rd, Banka TR, van Holsbeeck M. 2011 Mid-America Orthopaedic Association Dallas

B. Phemister Physician in Training Award. Can musculoskeletal tumors be diagnosed with ultrasound fusion-guided biopsy? Clin Orthop Relat Res 2012;470:2280–7.

[24] Schlaier JR, Warnat J, Dorenbeck U, Proescholdt M, Schebesch KM, Brawanski A. Image fusion of MR images and real-time ultrasonography: evaluation of fusion accuracy combining two commercial instruments, a neuronavigation system and a ultrasound system. Acta Neurochir (Wien) 2004;146:271–7.

[25] Yang EY, Polsani VR, Washburn MJ, et al. Real-time co-registration using novel ultrasound technology: ex vivo validation and in vivo applications. J Am Soc Echocardiogr 2011;24:720–8.

[26] Sofuni A, Itoi T, Itokawa F, et al. Real-time virtual sonography visualization and its clinical application in biliopancreatic disease. World J Gastroenterol 2013;19:7419–25.

[27] Wilasrusmee C, Pongchairerks P. Pancreaticobiliary ductal anatomy in Thai people. J Hepatobiliary Pancreat Surg 1999; 6:79–85.

[28] Schulz HG, Christou A, Gursky S, Rother P. Computerized tomography studies of normal morphology and volumetry of parenchymatous epigastric organs in humans. Anat Anz 1986;162:1–12.

[29] Pochhammer KF, Székessy T. Ultrasound and pancreatic length. Ultraschall Med 1982;3:2–3.

Figure legends

Figure 1. Volume Navigation system.

US was performed using a LogicE9 system (GE Healthcare) equipped with real time fusion imaging and GPS-like technology using a position sensor in the magnetic field. Magnetic field generator (arrow), Sensor (arrowhead).

US: transabdominal ultrasonography, GPS: global positioning system

Figure 2. Measurements of pancreatic length and blind area using GPS-like technology and CT-fusion imaging.

(a) CT fusion technique for direct comparison of the lesion in different modalities and depiction in any section. GPS markers were marked on both US and CT-fusion image. The size of square (□) means the distant from set position. The plus (+) means the corresponding with set position.

(b) GPS marker was marked at the center of the pancreatic parenchyma on the left side of the confluence of the splenic and superior mesenteric veins on CT-fusion image.

(c) The length of the pancreatic head (A); measured the length from the Vater papilla (the confluence of MPD and common bile duct) to GPS marker on CT-fusion image.

(d) The length of the pancreatic body and tail (B); measured the length from GPS marker to the edge of the pancreatic tail on CT-fusion image.

(e) The observable limitation point of the pancreatic tail on US (target point: TP-US) was marked by using position-sensor-function (left) and TP-CT was automatically marked on CT-fusion image (right).

(f) ①Real unobservable area of the pancreatic tail: RU; the length from TP-CT to the edge of the pancreatic tail was measured on CT-fusion image. ②Predictive length of unobservable area on US : PU-US ; the length from the splenic hilum to TP-US in left intercostal view was measured on US. ③Predictive length of unobservable area on CT : PU-CT; the length corresponding with PU-US was measured on CT-fusion image.

Figure 3. Visualization of the pancreatic tail from the splenic hilum region on US image.

The pancreatic tail was observed on US image while referring to target point (TP)-US, TP-CT and CT-fusion image in left intercostal scan and it was determined three types of view;

(a) The pancreatic tail was identified between TP-US and the splenic hilum,

(b) The pancreatic tail was not identified but the existence of it was suspected on US image,

(c) The pancreatic tail was not identified and the existence of it was not suspected due to gas in the intestinal tract.

Figure 4. Difference in the distance between TP of the estimators and TP of the examiner.

Target point (TP): Green cross was marked at the observable limitation point of the pancreatic tail on US by the examiner. Yellow and red circles were marked by other two expert gastroenterologists on US image only after the examination. The distances between the marks (yellow and red) of the two estimators and the cross mark (green) of the examiner were measured perpendicular to the direction of the long axis.

Figure 5. Correlation between measurement parameters and physical parameters.

Correlations with parameters were shown in these figures. RU with BMI (Pearson R=0.446, P=0.004) and waist circumference (R=0.354; P=0.027), PU-US with PU-CT (R=0.904; P<0.0001), and RU with PU-US (R=0.788; P<0.001).

Table 1

Clinical characteristics of the 39 Patients.

Case	Sex	Age,yr	Diagnosis	Tumor Size(mm)	Tumor Location	Diameter of MPD(mm)
1	Male	77	Pancreatic carcinoma	25	Body	<3.0
2	Female	66	IPMN	30	Head	<3.0
3	Female	59	IPMN	40	Head	3.0
4	Male	53	IPMN	22	Body	<3.0
5	Male	39	SPN	20	Body	<3.0
6	Male	68	Adenoma of the major duodenal papilla, POST	-	-	<3.0
7	Male	70	Adenoma of the major duodenal papilla, POST	-	-	<3.0
8	Female	58	IPMN	14	Head	3.0
9	Male	45	Adenoma of the major duodenal papilla, POST	-	-	<3.0
10	Male	41	Paraganglioma	-	-	<3.0
11	Female	79	Tumor of the major duodenal papilla, PRE	-	-	<3.0
12	Male	56	Cholelithiasis	-	-	<3.0
13	Female	71	IPMN	46	Body	4.6
14	Male	68	Cholelithiasis	-	-	<3.0
15	Male	61	Pancreatic carcinoma	14	Body	4.1
16	Female	72	Paraganglioma	-	-	<3.0
17	Female	80	Perihilar cholangiocarcinoma	-	-	<3.0
18	Male	56	Adenoma of the major duodenal papilla, POST	-	-	<3.0
19	Female	60	Tumor of the major duodenal papilla, PRE	-	-	<3.0
20	Female	48	Duodenal polyp	-	-	<3.0
21	Male	63	Tumor of the major duodenal papilla, PRE	-	-	<3.0
22	Male	70	Adenoma of the major duodenal papilla, POST	-	-	<3.0
23	Male	62	Adenoma of the major duodenal papilla, POST	-	-	<3.0
24	Male	75	Mass forming pancreatitis	27	Head	<3.0
25	Male	36	Pancreatic carcinoma	18	Head	4.9
26	Female	77	Cholecystitis	-	-	<3.0
27	Female	47	Tumor of the major duodenal papilla, PRE	-	-	<3.0
28	Female	69	Gallbladder carcinoma	-	-	<3.0
29	Female	73	IPMN	10	Body	3.5
30	Female	75	Gallbladder carcinoma	-	-	<3.0
31	Female	66	IPMN	40	Head	3.5
32	Male	71	Pancreatic carcinoma	20	Head	3.9
33	Male	58	Pancreatic carcinoma	45	Head	<3.0
34	Male	76	Adenoma of the major duodenal papilla, POST	-	-	3.3

35	Female	63	Pancreatic carcinoma	10	Body	4.7
36	Male	63	Cholecystitis	-	-	<3.0
37	Male	56	Cholecystitis	-	-	<3.0
38	Female	46	GIST of duodenum	-	-	<3.0
39	Female	77	Cholecystitis	-	-	<3.0

IPMN, intraductal papillary mucinous neoplasm; SPN, Solid-pseudopapillary neoplasm; GIST, gastrointestinal stromal tumor; MPD, main pancreatic duct; PRE, pre papillectomy; POST, post papillectomy

Table 2

US findings with GPS-like technology and CT fusion of the 39 patients.

US findings	Total (n = 39)	Male (n= 21)	Female (n = 18)	*P* value	No dilatation of MPD(n=29)	Dilatation of MPD(n=10)	*P* value
Real pancreatic length (mm)	160.9±16.4	165.4±16.3	155.6±15.3	0.061	162.6±17.3	155.7±12.5	0.25
RU(mm)	41.0±17.8	45.0±16.7	36.4±18.3	0.133	42.0±18.3	38.3±16.8	0.58
UA(%)	25.3±10.4	27.1±9.3	23.2±11.5	0.260	25.5±10.6	24.6±10.5	0.81
PU-US(mm)	52.0±15.8	57.3±13.6	45.8±16.2	0.021[a]	52.0±15.0	52.1±18.8	0.98
PU-CT(mm)	52.6±16.4	59.0±14.1	45.5±16.6	0.010[a]	55.4±16.2	45.0±15.9	0.10

RU, real unobservable length of the pancreatic tail; UA, unobservable area (The ratio of RU to the real pancreatic length); PU, predictive length of the unobservable area [a] *t*-test

Table 3

US findings in 39 cases of the pancreatic tail in left intercostal scan.Three types of US findings.

	Type of US findings		n=39 (%)
Observable	a	Identified	13 (33)
	b	Not identified, but suspected	9 (23)
Unobservable	c	Not identified	17 (44)

Figure 1

Click here to download high resolution image

Figure 2 a

Click here to download high resolution image

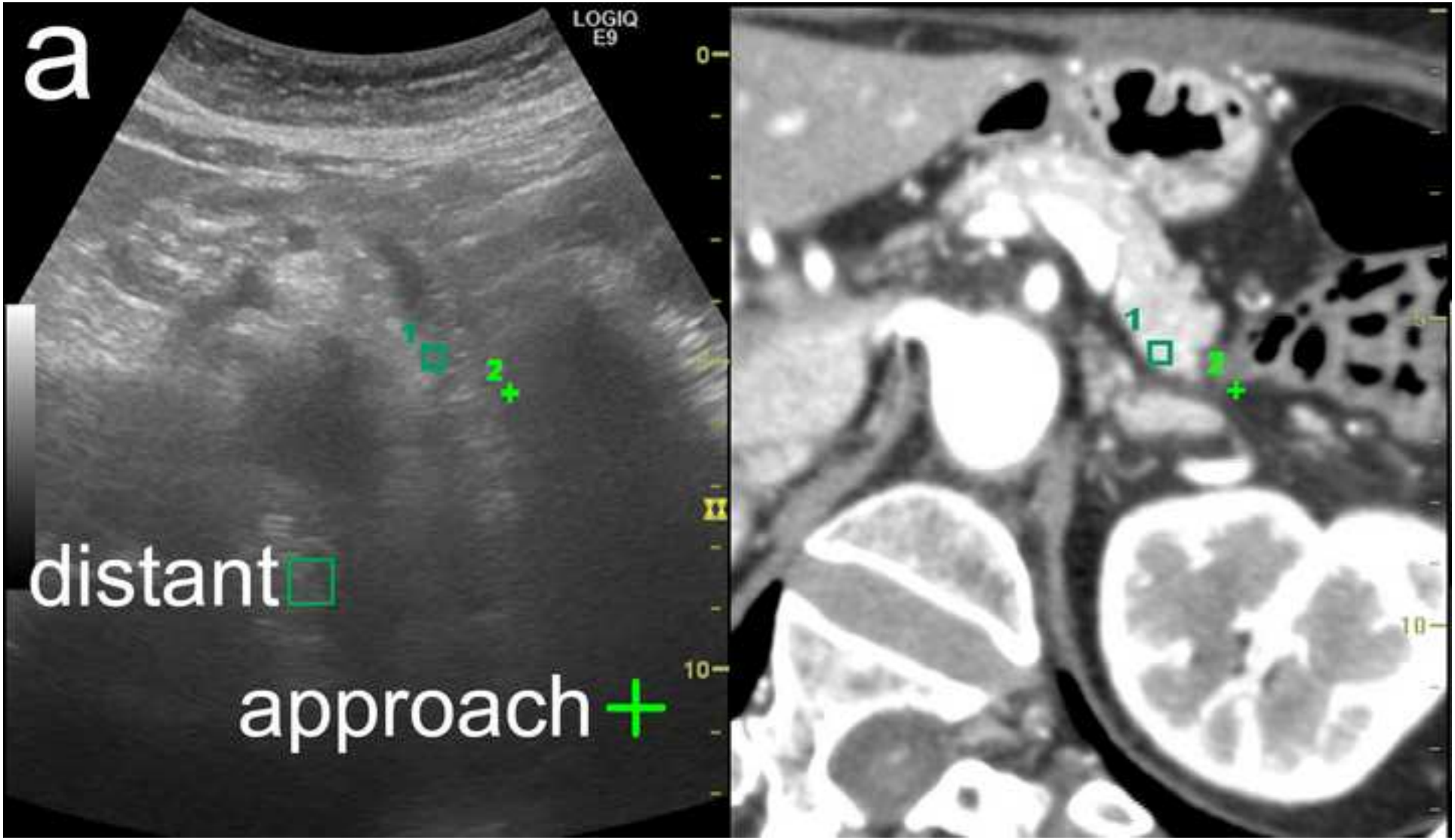

Figure 2 b

Click here to download high resolution image

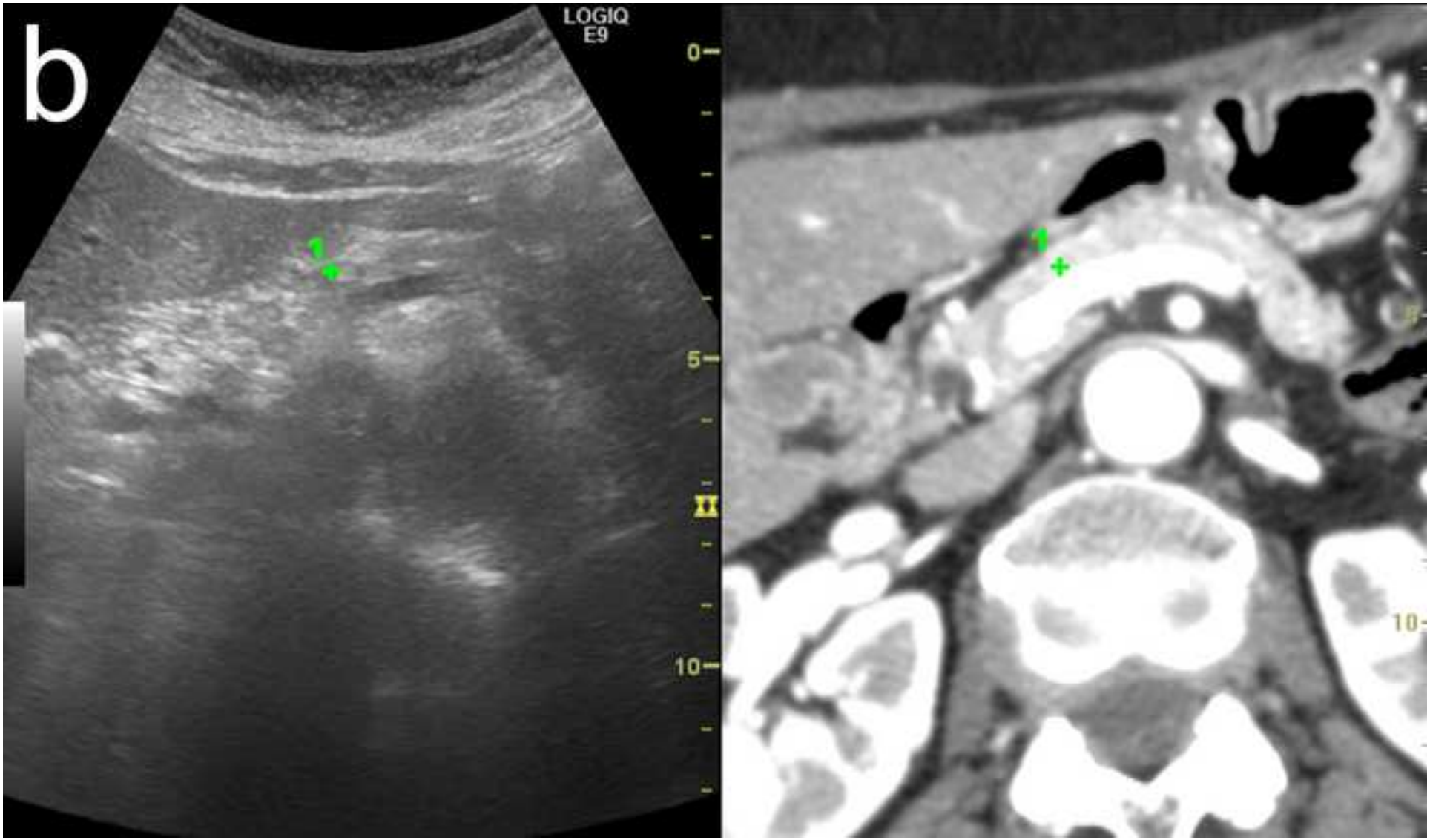

Figure 2 c

Click here to download high resolution image

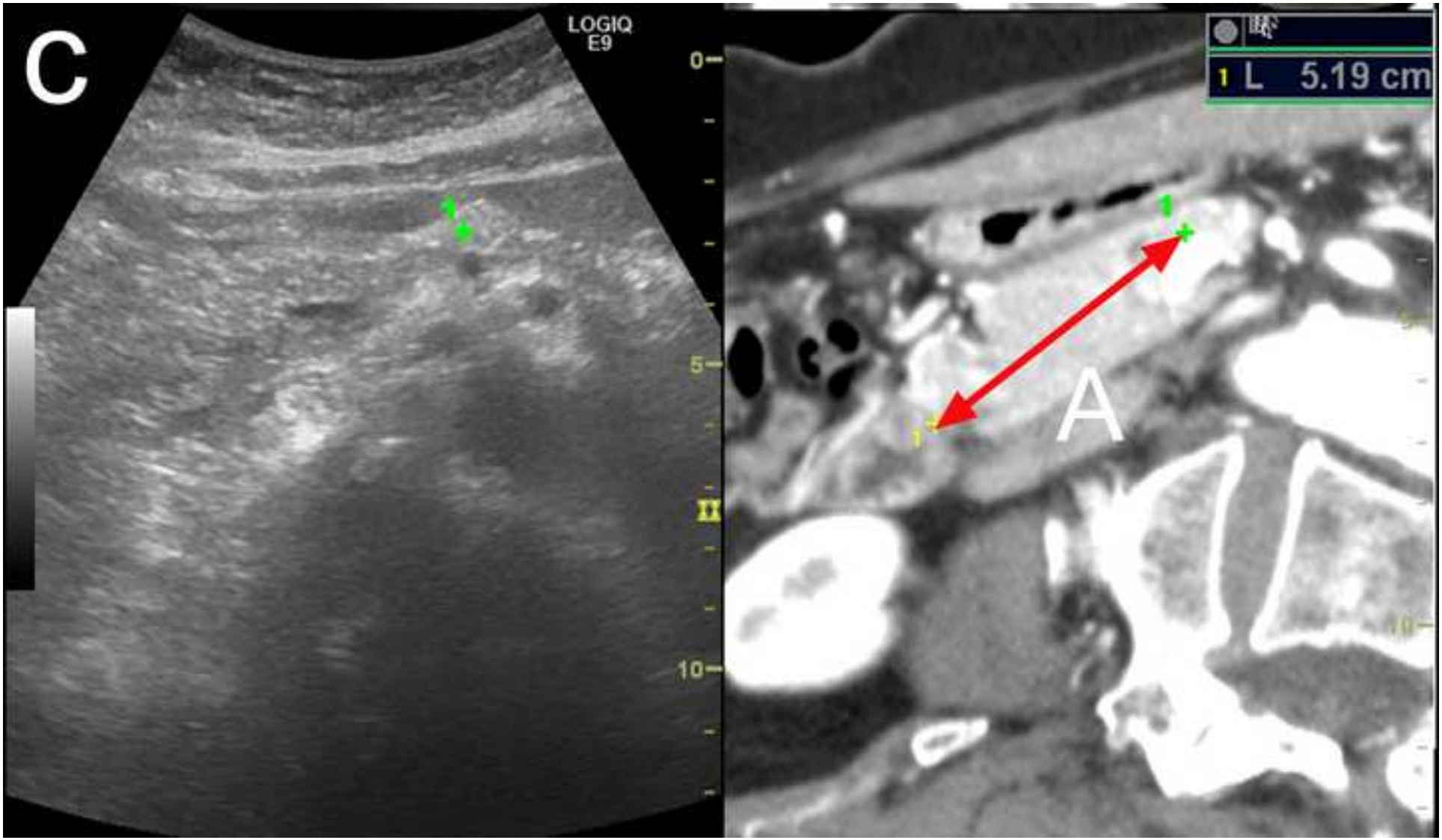

Figure 2 d

Click here to download high resolution image

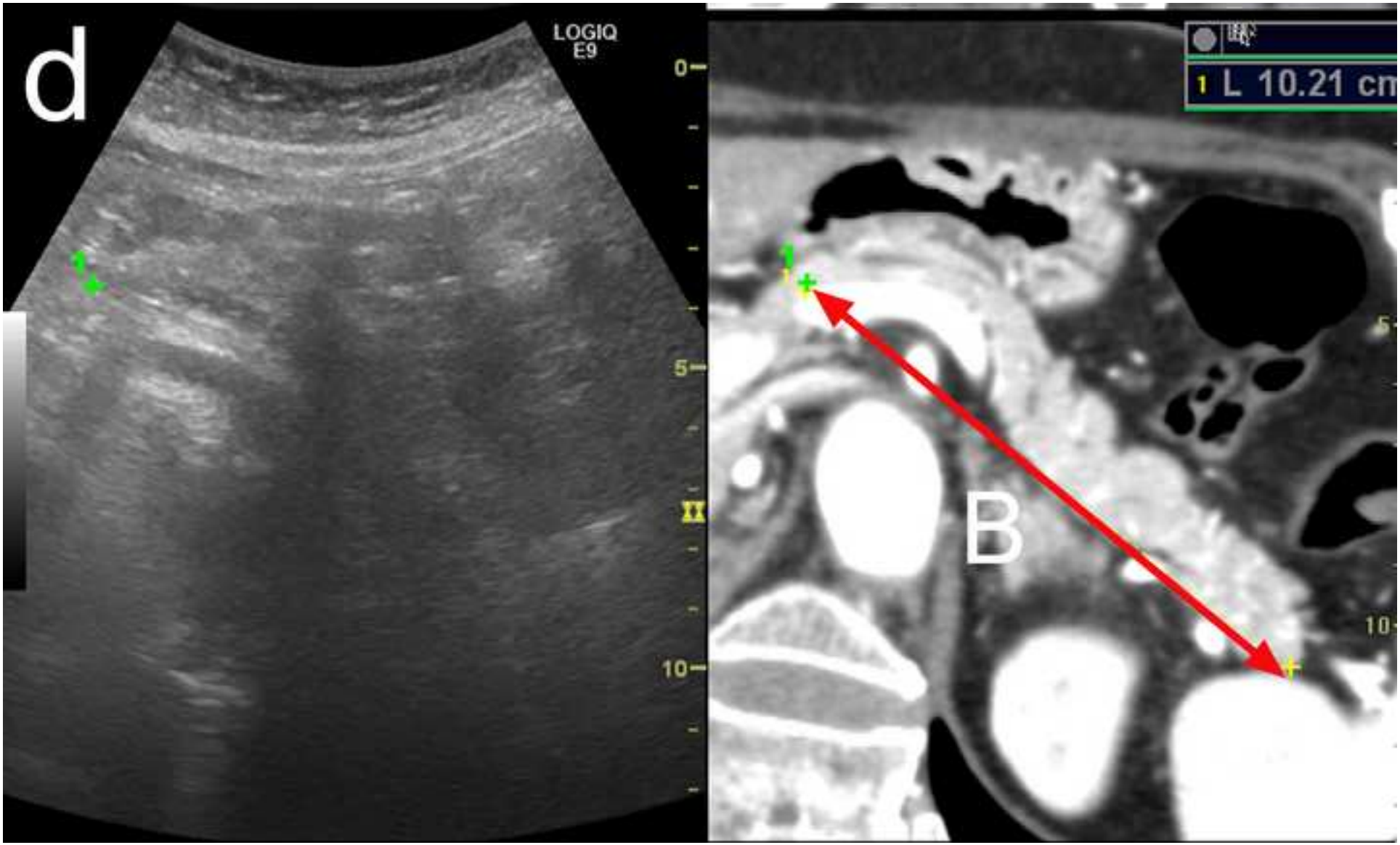

Figure 2 e

Click here to download high resolution image

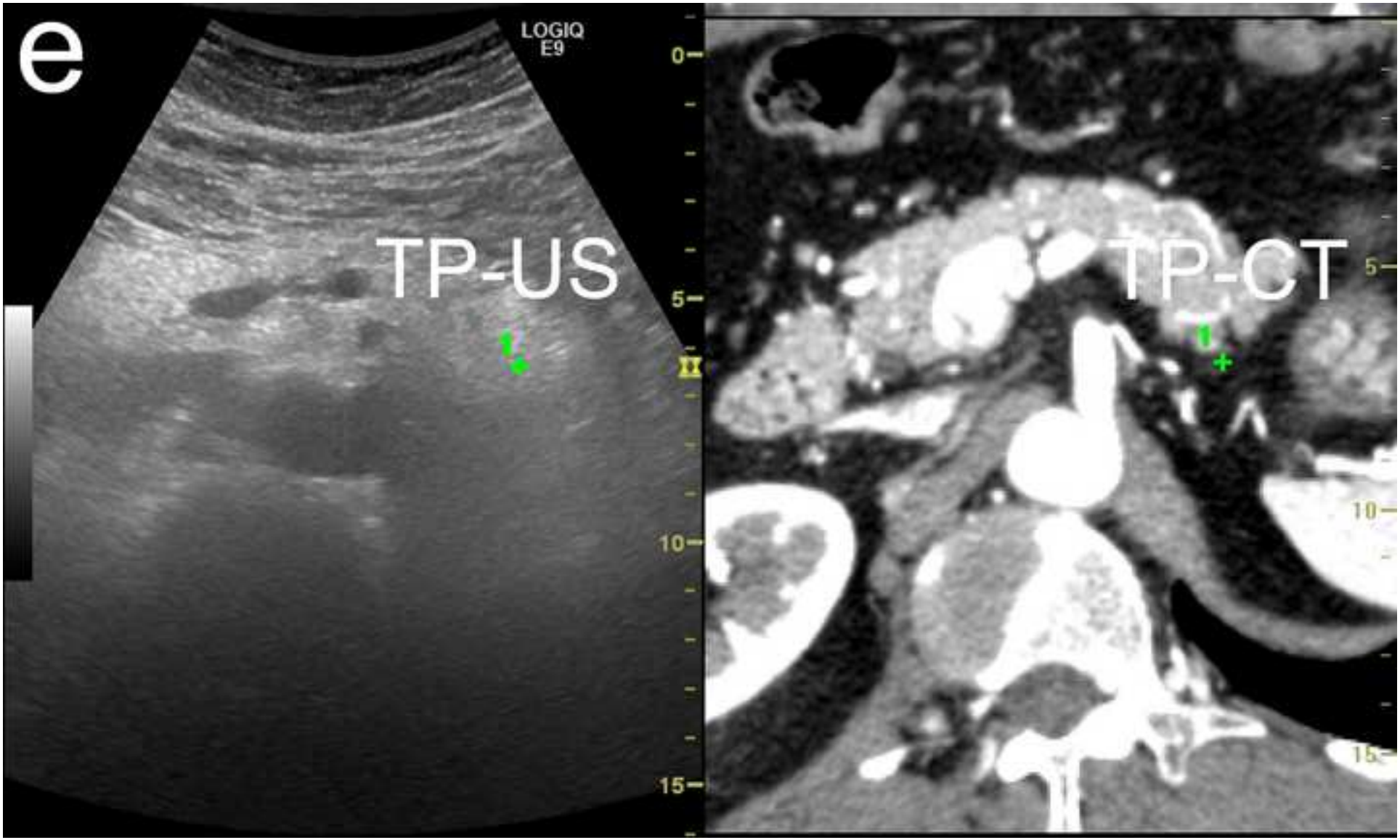

Figure 2 f

Click here to download high resolution image

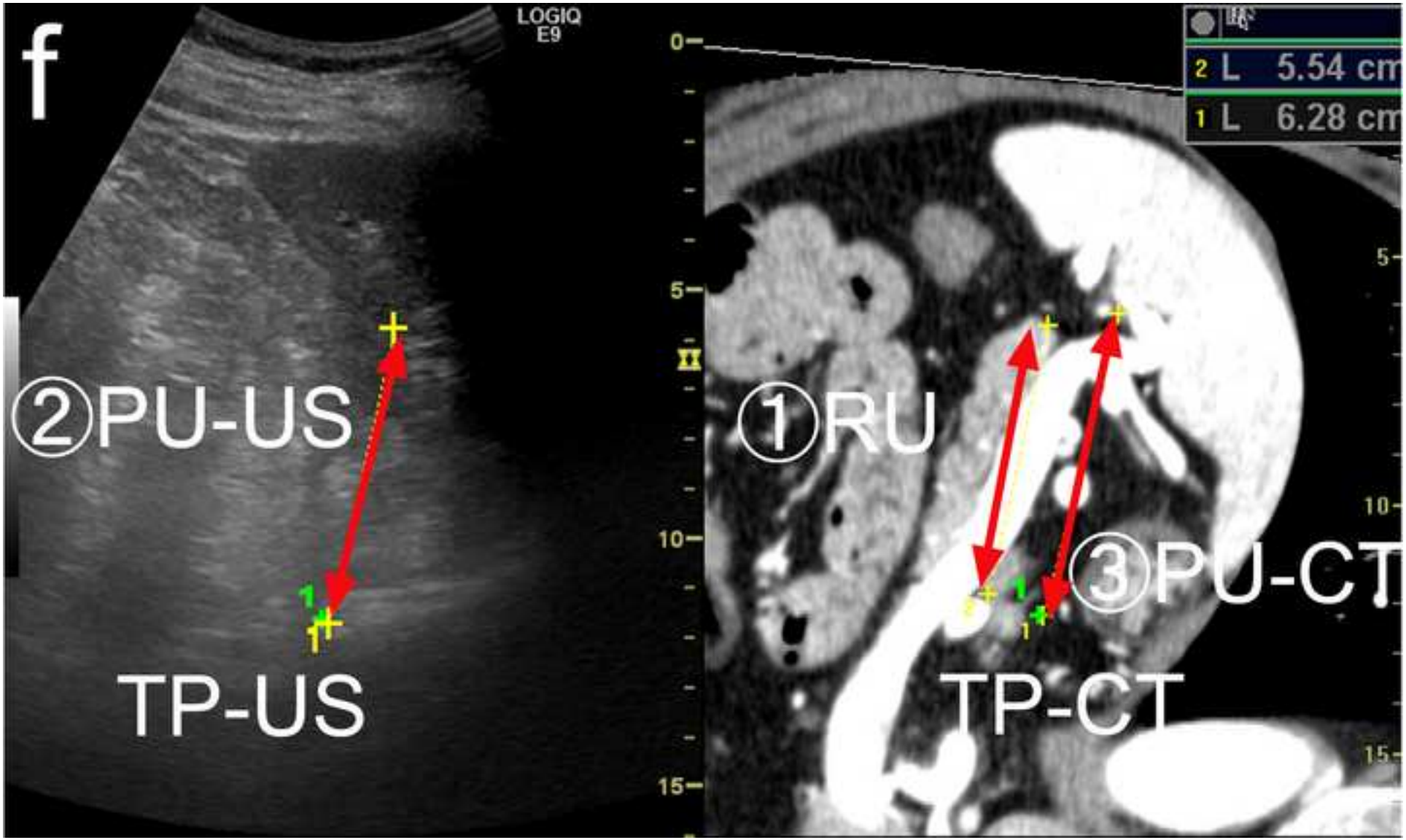

Figure 3 a

Click here to download high resolution image

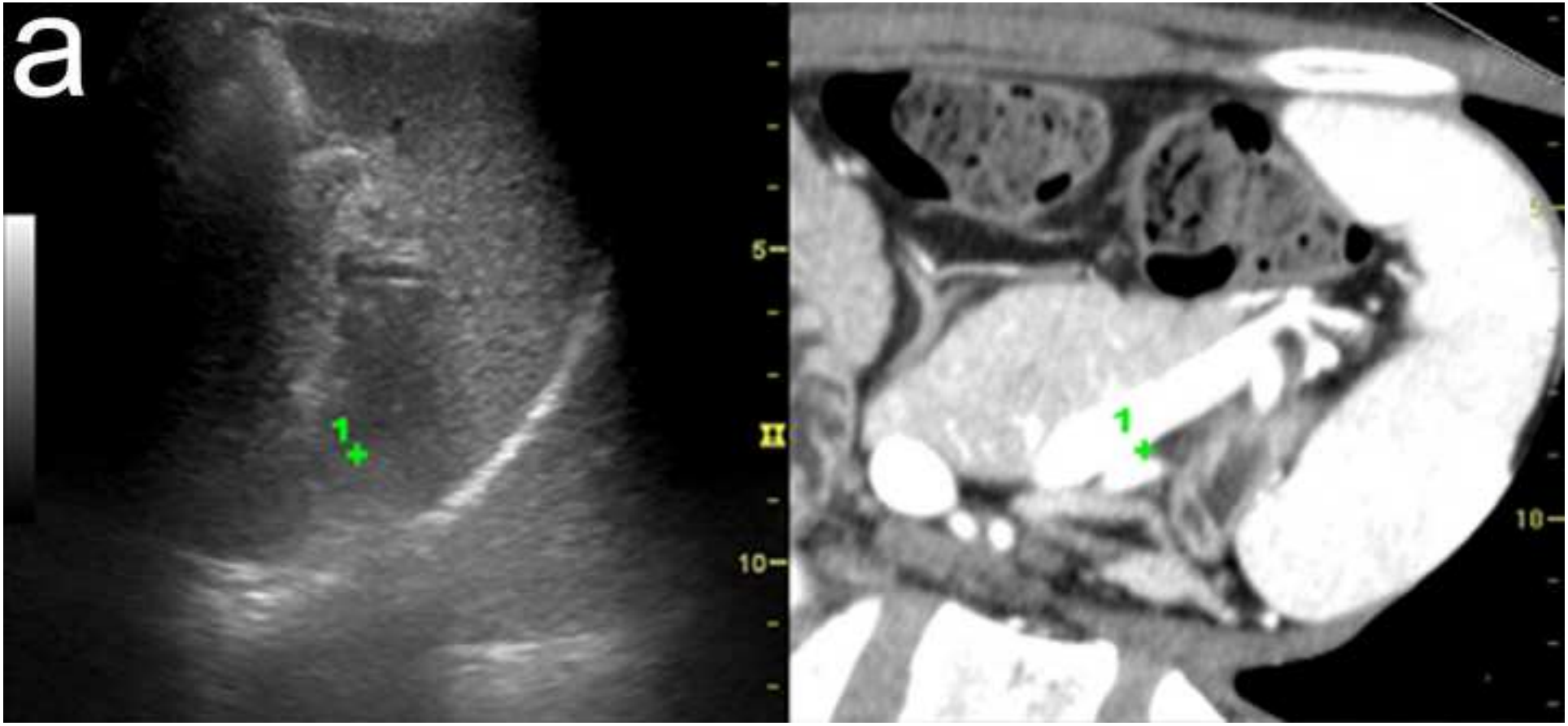

Figure 3 b

Click here to download high resolution image

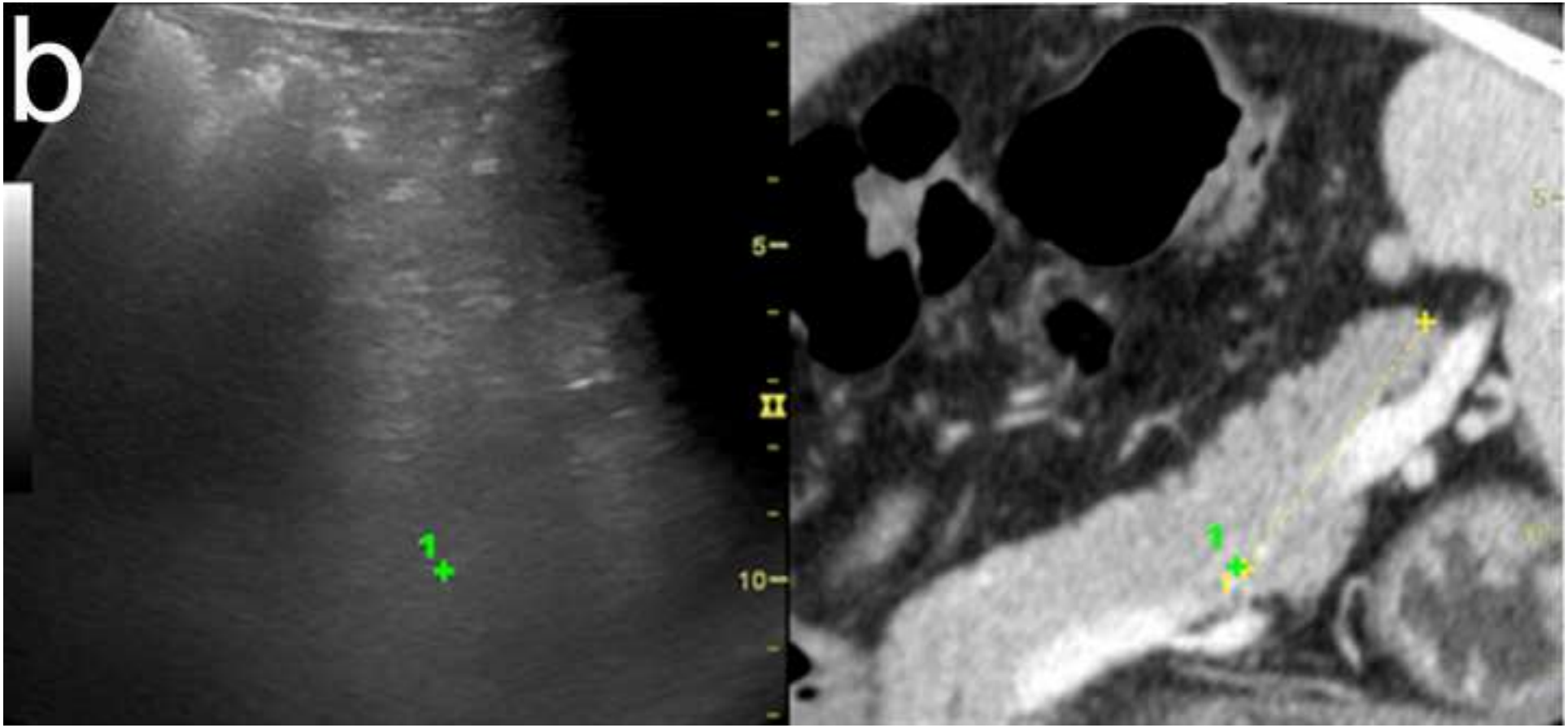

Figure 3 c

Click here to download high resolution image

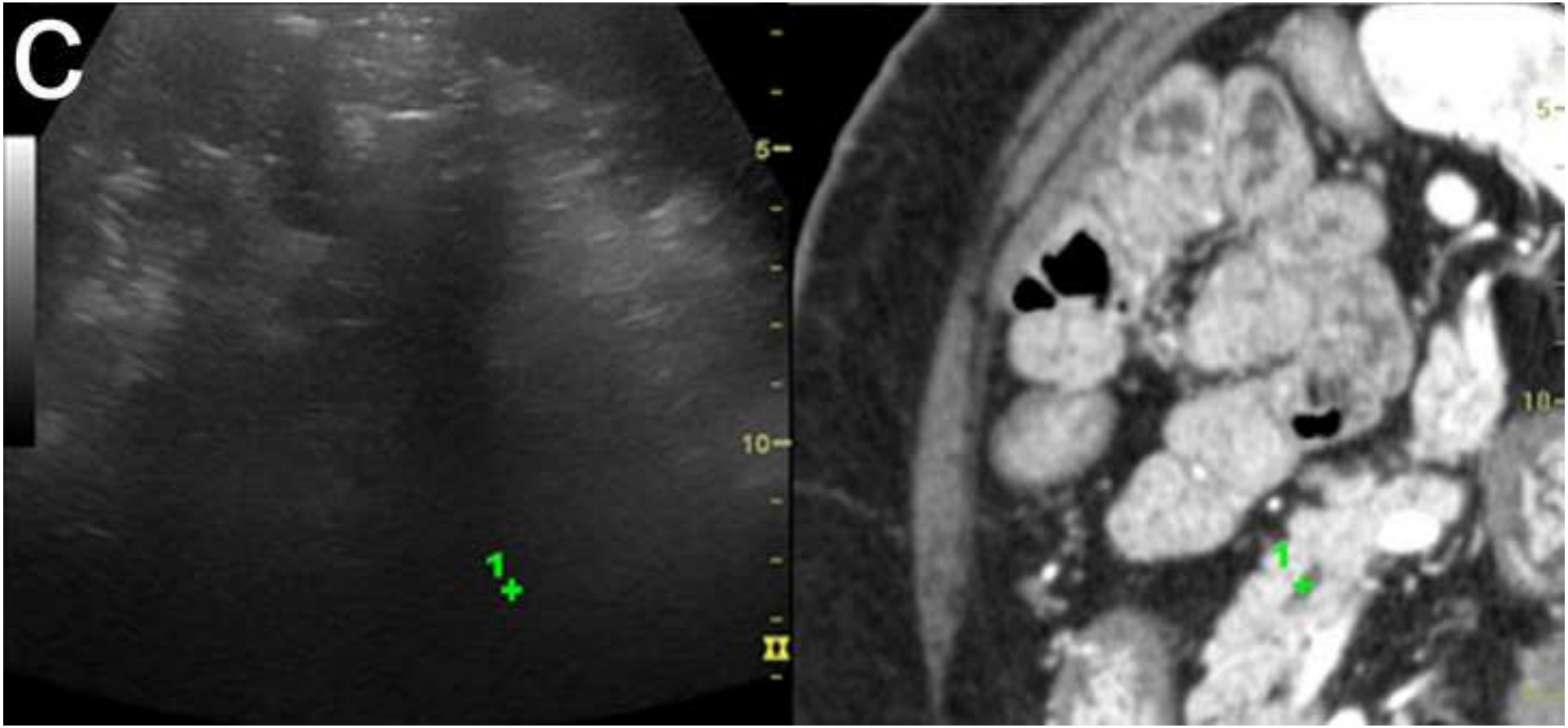

Figure 4

Click here to download high resolution image

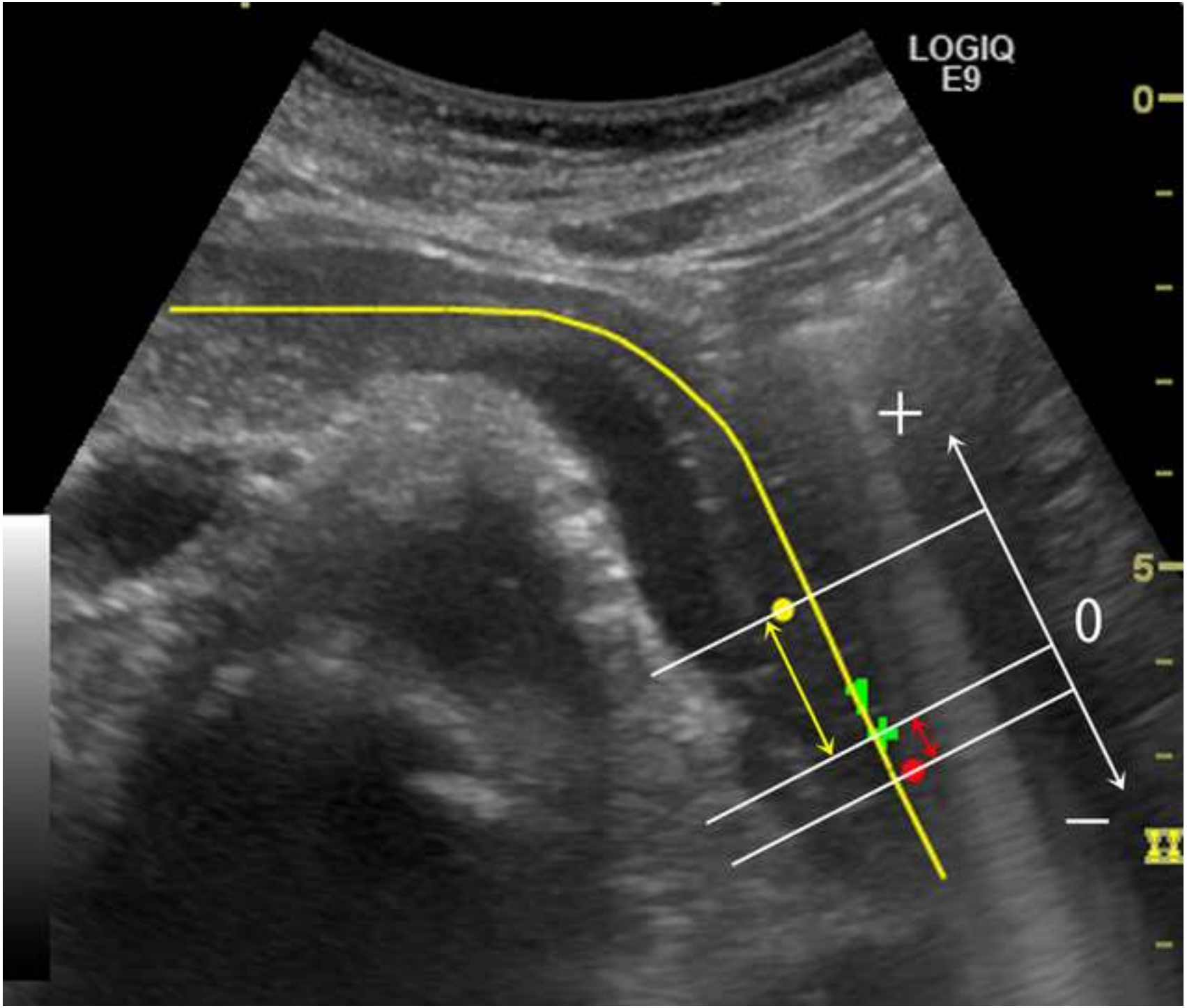

Figure 5

Click here to download high resolution image